Emerging technologies for image guidance and device navigation in interventional radiology

George C. Kagadis[a)]
Department of Medical Physics, School of Medicine, University of Patras, P. O. Box 132 73, GR 265 04 Rion, Greece

Konstantinos Katsanos
Department of Interventional Radiology, Guy's and St.Thomas' Hospitals, NHS Foundation Trust, King's Health Partners, London SE1 7EH, United Kingdom

Dimitris Karnabatidis
Department of Radiology, School of Medicine, University of Patras, Rion GR 265 04, Greece

George Loudos
Department of Medical Instruments Technology, Technological Educational institute of Athens, Ag. Spyridonos Street, Egaleo GR 122 10, Athens, Greece

George C. Nikiforidis
Department of Medical Physics, School of Medicine, University of Patras, Rion GR 265 04, Greece

William R. Hendee
Department of Radiology, Mayo Clinic, Rochester, Minnesota 55905

(Received 10 April 2012; revised 7 August 2012; accepted for publication 7 August 2012; published 4 September 2012)

Recent developments in image-guidance and device navigation, along with emerging robotic technologies, are rapidly transforming the landscape of interventional radiology (IR). Future state-of-the-art IR procedures may include real-time three-dimensional imaging that is capable of visualizing the target organ, interventional tools, and surrounding anatomy with high spatial and temporal resolution. Remote device actuation is becoming a reality with the introduction of novel magnetic-field enabled instruments and remote robotic steering systems. Robots offer several degrees of freedom and unprecedented accuracy, stability, and dexterity during device navigation, propulsion, and actuation. Optimization of tracking and navigation of interventional tools inside the human body will be critical in converting IR suites into the minimally invasive operating theaters of the future with increased safety and unsurpassed therapeutic efficacy. In the not too distant future, individual image guidance modalities and device tracking methods could merge into autonomous, multimodality, multiparametric platforms that offer real-time data of anatomy, morphology, function, and metabolism along with on-the-fly computational modeling and remote robotic actuation. The authors provide a concise overview of the latest developments in image guidance and device navigation, while critically envisioning what the future might hold for 2020 IR procedures. © *2012 American Association of Physicists in Medicine*. [http://dx.doi.org/10.1118/1.4747343]

Key words: image guidance, device navigation, robotic technologies, interventional radiology

I. CURRENT STATUS OF STATIC AND REAL-TIME IMAGE GUIDANCE

Interventional radiology (IR) encompasses a wide range of image-guided diagnostic and therapeutic procedures. Interventional radiology procedures have been at the forefront of medical innovation during the past few decades due to the rapid adoption of technological developments in imaging and device miniaturization. Minimally invasive percutaneous and endovascular IR procedures have produced a major change in the treatment of the world's greatest killers, cardiovascular disease and cancer. Medical imaging is the "sine qua non" of IR; appropriate, high-quality imaging is essential for the successful execution of IR procedures.[1] As examples, static or real-time image-guidance is employed (a) for the advancement of fine wires and catheters inside human vessels and organs such as the gastrointestinal track and urinary system, (b) for the navigation and actuation of sophisticated instrumentation in procedures such as tumor radiofrequency ablation, balloon angioplasty, stent placement, and directional atherectomy, and (c) for the targeted delivery of active agents such as coils for embolization of traumatic lacerations and aneurysms, microparticles for the obliteration of hypervascular lesions such as fibroids and tumors, and delivery of drug payloads for tumor chemoembolization and intra-arterial thrombolysis.[1,2]

Current modes of image guidance for routine IR procedures include but are not limited to digital subtraction angiography, c-arm fluoroscopy, cone-beam computed tomography (CBCT), multidetector computed tomography (MDCT), CT fluoroscopy, magnetic resonance imaging (MRI), ultrasonography (US), optical imaging, and multiple combinations

thereof. Nuclear medicine techniques of combined positron emission tomography and CT (PET/CT), or combined single photon emission computed tomography and CT (SPECT/CT), may also have an expanding role in future image-guided therapies, as technologies of image fusion and integration continue to develop.[1] The primary mode of choice depends on the target organ, the disease, and the type and function of the devices to be employed for treatment. Static cross-sectional image-guidance such as CT with high spatial resolution has traditionally been used for percutaneous solid organ interventions such as tissue biopsy and thermal ablation treatments, whereas real-time fluoroscopy and angiographic roadmapping are necessary for endovascular procedures such as aortic graft placement, transluminal angioplasty, and arterial embolization. In principle, diagnostic services prioritize high-quality imaging, whereas interventional therapies emphasize real-time imaging with reduced radiation burden. For safety reasons, x-ray exposure during an IR procedure is restricted to the region of interest, and an acceptable tradeoff must be made between resolution and dose for real-time imaging.[1,2] It is noteworthy that the science and technology for understanding and implementing those tradeoffs is an area of ongoing work, but their analysis is beyond the scope of the present paper.

During most interventional procedures, image guidance must fulfill four key roles as stated by Solomon *et al.*:[1] (1) detailed preprocedural planning (i.e., review of baseline imaging to plan the intervention); (2) accurate intraprocedural targeting (i.e., to advance the needle, wire, or catheter to the desired anatomic target); (3) intraprocedural monitoring of the treatment and its immediate outcomes or complications (i.e., monitor tissue changes caused by the delivered treatment and make any necessary adjustments of the interventional tools); and (4) postprocedural assessment of the treatment results (i.e., evaluate the results of the procedure and the need for additional therapy). Traditionally, the first and fourth role belong to diagnostic imaging, but newer image fusion technologies are blurring the borders between diagnostic and interventional imaging, and modern image-guided therapeutic approaches may blend data from several sources across time and space. Nonetheless, real-time imaging feedback is necessary during the second and third step so that the interventionalist may accurately target the diseased vessel or organ, effectively operate or actuate the interventional technologies, and monitor immediate outcomes while screening for complications. Within the context of the present paper, the authors define real-time image guidance for interventional radiology as dynamic imaging that is synchronous with the interventional procedure and has temporal resolution sufficient to provide feedback within a reasonable time window so that the interventionalist can safely and effectively accomplish the desired procedural task. The necessary time window will depend on the actual procedure. For example, x-ray guided endovascular procedures warrant real-time imaging with multiple frame acquisitions per second (subsecond temporal resolution), whereas near real-time imaging with a latency of a few seconds may suffice for MR-guided tumor ablation.

Several different disciplines may have access to cross-sectional and angiographic imaging equipment in a modern healthcare institution, including state-of-the-art facilities for performance of IR procedures in dedicated interventional suites and high-end hybrid operational theatres. Recent innovations in image-guidance and device navigation, along with emerging robotic actuation technologies, are rapidly transforming the landscape of IR practice. In this paper the authors provide a concise overview of the latest developments, and a projection of what the future may hold for IR procedures.

II. DEVELOPMENTS IN IMAGE GUIDANCE TECHNOLOGIES

II.A. Multimodality image registration and fusion

For a patient scheduled for a minimally invasive radiological treatment, preprocedural evaluation may involve several imaging examinations to confirm the diagnosis and to aid the planning of treatment, thereby increasing the safety and effectiveness of the procedure. During treatment planning the physician is expected to review baseline imaging studies, confirm that the intended treatment is indicated, and plan the route of interventional access so catheters, wires, electrodes, or other technologies can be safely and easily advanced to the target without serious risks to nearby anatomical structures. The volume of baseline data may span thousands of cross-sectional CT and MR images acquired with a variety of algorithms and contrast agents. Utilization of these data could have a major impact on real-time monitoring of the application and performance of the image-guided treatment, while at the same time reducing patient exposure to ionizing radiation and increasing the throughput of interventional procedures.[3]

Future state-of-the-art IR procedures will likely include real-time imaging that displays the target, interventional devices, and surrounding anatomy in three dimensions, and combines anatomical (i.e., tissue morphology) and functional information (i.e., organ perfusion and metabolism) to monitor treatment and to control outcomes and potential complications. Multimodality image fusion will be needed to accomplish this task, because there is no single modality available with such combined imaging features. Image registration is generally defined as the process of bringing two image datasets into spatial alignment, whereas image fusion is defined as the integration of different image data into a new single image. The process of image registration can be formulated as a challenge of optimizing a function that quantifies the match between the original and the transformed image.[4–6] Intermodality or intramodality image registration provides an imaging framework for IR guidance. Image registration between two-dimensional (2D) or three-dimensional (3D) images is a common challenge encountered when more than one image of the same anatomical structure are obtained, either using different anatomical imaging modalities or performing dynamic studies. In all cases, the information present in the images must be combined to produce superimposed fused images. Image registration algorithms may be manual and operator-dependent, semiautomatic, or automatic. Image

registration may be rigid or elastic, in which case some image deformation is allowed to improve image correspondence. Of note, image fusion may or may not have accounted for deformation between the included images. For example, in the case of fusion of US images with CT or MR, there is typically no account of deformation imparted by the US transducer. Deformable models with elastic matching algorithms have been introduced to correct for organ motion due to respiration, cardiac motion, and aortic pulsation, thereby achieving more accurate and realistic image registration and fusion.[7]

Diagnostic imaging systems such as PET/CT, SPECT/CT, and PET/MR represent the benchmark of image fusion technologies. In a similar fashion, overlay of PET datasets on MR or CT datasets allows the use of both anatomic and functional imaging data during image-guided therapies.[8–11] Multimodality image fusion may involve any combination between anatomic modalities (MR, CT, or US) and metabolic nuclear imaging (PET or SPECT). For enhanced radiological guidance during IR procedures one trend is to combine high-resolution cross-sectional MR or CT with real-time, radiation-free US (Fig. 1). It is also reasonable to combine a low-sensitivity modality that offers high spatial resolution and tissue contrast (MR or CT) with a nuclear modality that has low spatial resolution but high sensitivity (PET or SPECT).[1,12] In this manner, fusion of morphological and functional data can improve operator guidance and confidence during all phases of IR procedures. With the ongoing development of novel tracers, targeted molecular imaging techniques such as PET-CT and SPECT-CT are being used increasingly in the planning of cancer treatments and could become intricately linked in the future with image-guided therapies for a number of patient conditions.[13]

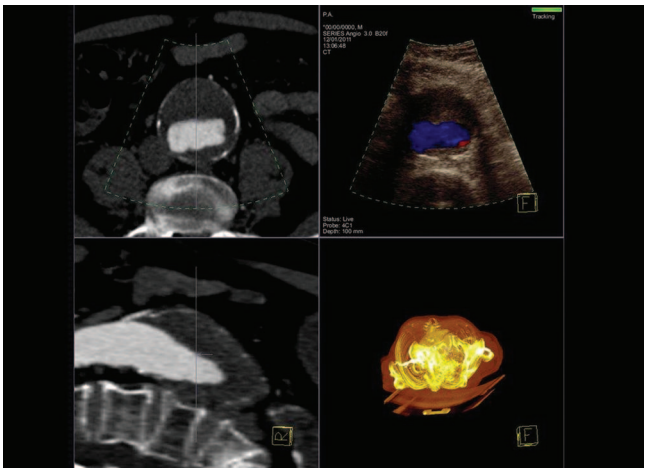

FIG. 1. Example of CT/US image fusion during preoperative evaluation of a patient with an abdominal aortic aneurysm. The patient had already experienced a thin-section contrast-enhanced CT scan. The patient-specific volumetric CT dataset was loaded into the ultrasound unit and the interlocking of cross-sectional CT images with corresponding real-time US images (image registration) was automatically performed in a few seconds by proprietary software-embedded without human interaction or external fiducial placement. The image registration process automatically updates and recalibrates the coregistered data to adjust for patient movement when necessary. The operator performs a transabdominal ultrasound scan of the aortic aneurysm in color Doppler mode (top right: sonography image with blood flow within the aneurysm) and the software updates and portrays the corresponding matched CT image in real-time and on the same screen (top left: corresponding axial contrast-enhanced CT image). As the operator scans the patient, further reconstructed CT views are provided for reference and orientation. (Bottom left: reconstructed midline sagittal CT image of the aneurysm shows the scanning level, bottom right: volume rendered image reconstruction of the imaged body segments; the chest and abdomen in this occasion) Innovations such as this may allow for exploitation of baseline CT scans with high anatomical detail during ultrasound-guided interventions, such as, during real-time ultrasound-guided puncture of the aneurysmal sac in order to treat an ongoing endoleak. Image courtesy of Siemens Healthcare, Germany (The eSie® image fusion platform; reproduced with permission).

Overlay of FDG-PET images that show tissue avidity (i.e., tracer uptake by the tissues of interest) onto cross-sectional anatomic images can provide critical information for the turnover of tumor metabolism and guide treatment with high precision in cases of small tumors or satellite recurrences following thermoablative treatments. The latter avenue was explored recently in an elegant investigation where researchers evaluated the combination of electromagnetic device tracking for image registration and subsequent CT/US/PET image fusion for near real-time image guidance during percutaneous and intraoperative biopsies and liver radiofrequency ablation.[14] Successful image fusion of coregistered US/CT with FDG PET scans was achieved in all patients. Thirty-one out of 36 biopsies were diagnostic, and RF ablation resulted in disappearance of FDG uptake in all cases after a mean followup treatment of almost 2 months.

II.B. Computational fluid dynamics and thermal modeling

Image fusion in IR may also include virtual images developed by sophisticated mathematical algorithms to simulate expected treatment outcomes and assist with treatment planning. For example, computational fluid dynamics (CFD) can provide realistic virtual images of blood hemodynamics across an aortic aneurysm or dissection.[15,16] CFD studies model realistic flow patterns and may simulate expected outcomes in order to influence therapeutic decision-making before correction with endovascular graft placement or surgery (Fig. 2).

Another example is treatment planning of thermal ablation therapies by computational thermal modeling [computational heat transfer (CHT)] of projected thermal lesions during radiofrequency or microwave ablation. Prototype computer software can predict the ablation volume according to prespecified electrode properties, and can superimpose virtual images of overlapping ablations on the tumor. This capacity allows the operator to choose an appropriate access route and determine how many ablations are needed to achieve complete destruction of the tumor.[17–19] Ellipsoid lesions simulating isotherms across tissue (i.e., estimations of tissue volumes at the same temperature) are drawn around imaginary electrodes, permitting the operator to rehearse the procedure and predict degrees of ablation by testing a variable number of electrodes, access routes, and electrode placements. The virtual thermal lesions (isotherms $>55\,^{\circ}C$)

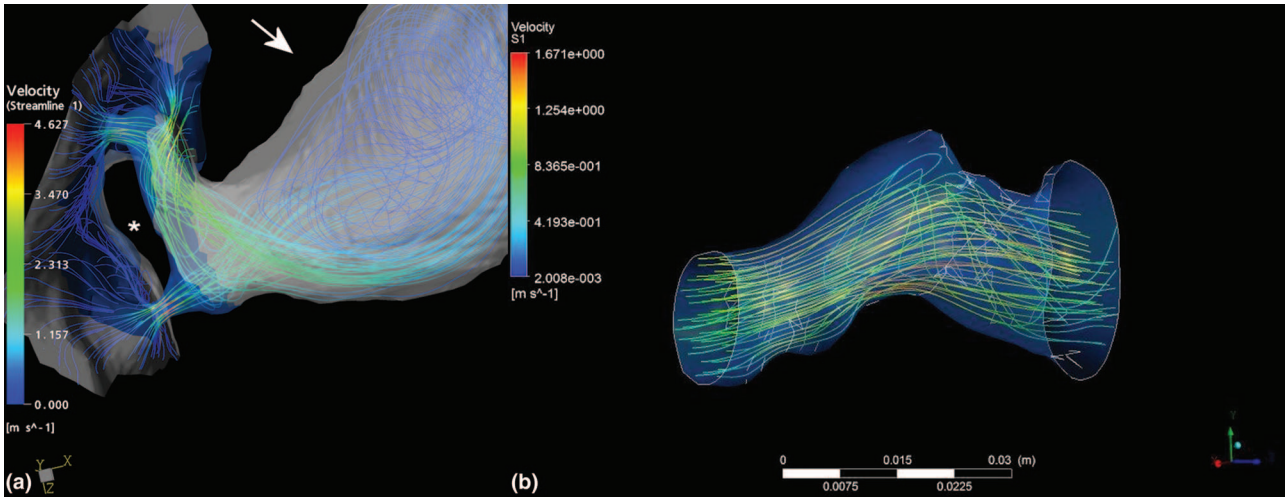

FIG. 2. Computational fluid dynamics modeling. (a) Streamlines across an ostial renal artery stenosis (complex high-grade stenosis indicated with white asterisk). Vessel segmentation was based on thin-section contrast-enhanced CT angiography. Note the vortices formed (arrow) after the high-grade stenosis. Reproduced with permission from Kagadis *et al.*, Medical Engineering & Physics **30**, 647–660 (2008). Copyright © 2008 Elsevier. (b) Streamlines in a segmented OCT acquired femoral artery. CFD mathematical models may be overlaid on three-dimensional anatomical models produced by CT, OCT, or MR to combine morphology with function during image-guided therapies. Hemodynamic parameters produced by CFDs may aid treatment planning and execution by pin-pointing areas of disturbed blood flow that have been linked to increased risk of thrombosis or restenosis after treatment. Direction of the flow is from left to right in both image parts.

are fused with the patient's baseline CT scan to identify potential sites of insufficient treatment and to avoid sensitive organs at risk. Computational thermal modeling may not only predict heat transfer and produce color-coded isothermal maps of treatment, it may also simulate additional steps such as vessel occlusion to minimize heat sinks or instillation of carbon dioxide or dextrose fluid to protect sensitive organs (Fig. 3).[6] Computational models of heat transfer are based on the Pennes bioheat equation of tissue-heat interactions, and projected outcomes may be estimated by traditional finite element analysis or other more novel approaches.[20]

II.C. Perfusion imaging and tissue thermometry

Perfusion imaging can be used in IR image guidance to provide a crude estimate of tissue perfusion as a surrogate endpoint of tissue viability and potential clinical success.[21] The endpoint may be either effective restoration of tissue perfusion during angioplasty procedures ischemic cardiovascular syndromes such as critical limb ischemia in diabetics or in patients with ischemic heart disease,[22–24] or elimination of tissue perfusion in cases of percutaneous tumor ablation in the liver, lung, and kidneys.[25] Tissue enhancement in contrast CT or MR, time-resolved CT or MR perfusion, noncontrast MR diffusion, arterial spin labeling MR, or microbubble-enhanced US have all been suggested as approaches to estimating tissue necrosis and residual tumor viability after targeted interventional oncological therapies.[1,26] Integration of functional parameters of perfusion imaging with x ray or US image guidance in the form of image fusion or intermittent treatment monitoring could become a useful addition to the array of standard image-guided modalities. Data derived from perfusion imaging can also be integrated into the tissue perfusion component of the Pennes equation in order to provide more realistic thermal modeling and treatment planning.[6]

Of particular interest in the field of interventional oncology is the development of CT- and MR-based approaches to tissue thermometry to provide intermittent or continuous real-time monitoring of tissue thermal properties. Visualization of tissue isothermal maps during interstitial tumor thermoablation using radiofrequency, microwave, or laser radiation is an elegant way of predicting tissue necrosis and therapy outcomes. Increasing use of these technologies in the future could provide more definitive endpoints of when the ablation is complete and the entire tumor has been successfully eradicated. In parallel, procedural safety will be increased by early identification of sensitive surrounding structures at risk of injury if exposed to an unnecessarily high dose of thermal energy.[27–29] In principle, tissue temperatures may be calculated with an accuracy of 1° because tissue proton resonance frequency varies with temperature.[30] By establishing a threshold of 55 °C–60 °C, or portraying the isothermal volumes as they develop during ablation, one can accurately predict the area of tissue thermocoagulation. At temperatures above 60 °C, instantaneous cell death and tissue coagulation occurs.[31]

CT and US parameters can also be exploited to measure tissue temperature. Temperature-dependent changes of CT tissue attenuation and ultrasonic velocity have been used to derive approximate tissue temperatures.[32,33] Temperature-dependent changes of tissue x-ray attenuation occur because tissue water has a coefficient of thermal density expansion of -3.6×10^{-4}/°C at human body temperatures. Based on the expansion coefficient, a linear relationship between voxel density in Hounsfield Units and tissue voxel temperature has

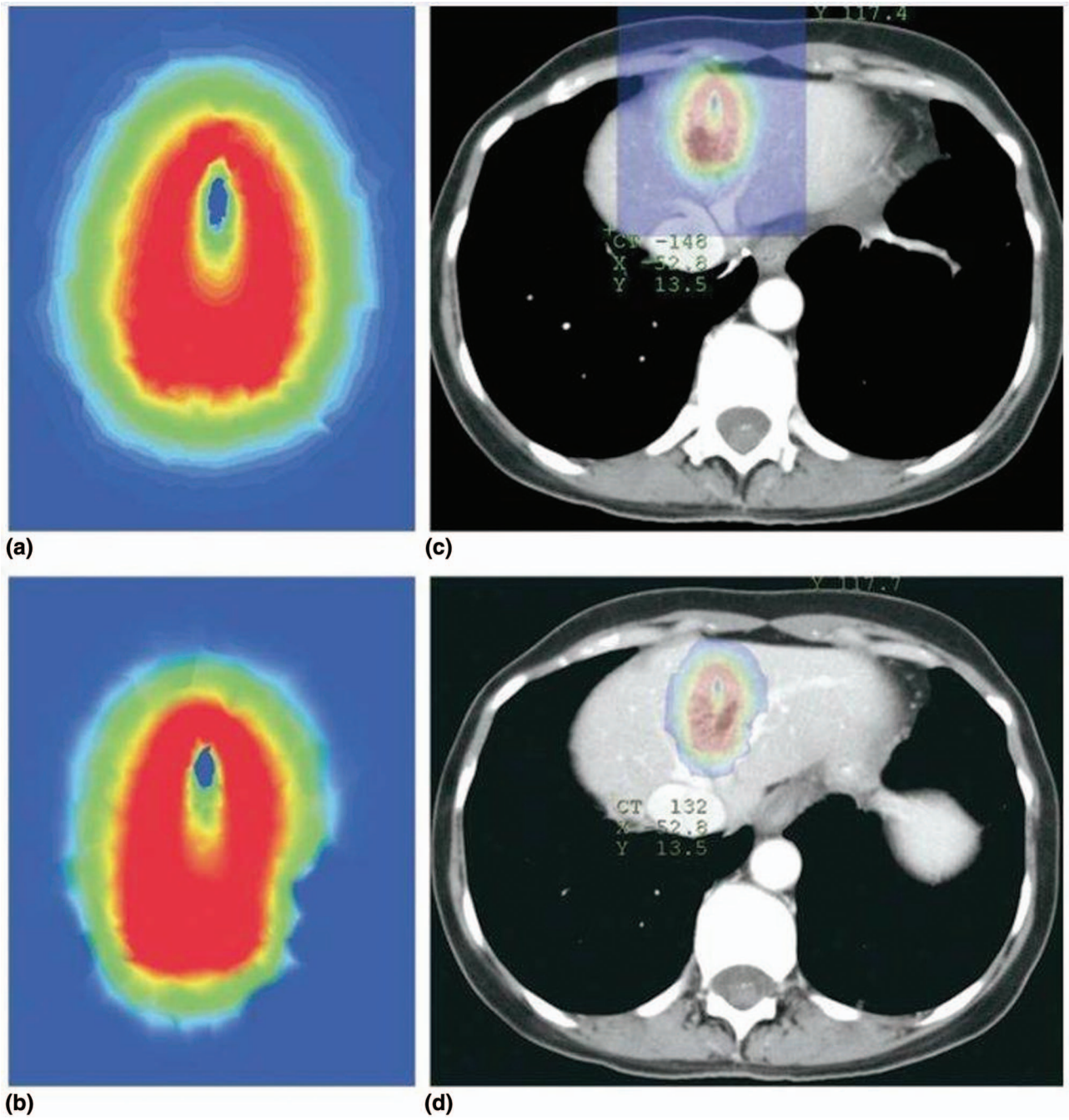

FIG. 3. Computational heat transfer modeling during thermal ablation. Isothermal areas are calculated and fused with the raw cross-sectional anatomy. (a) Simulated isothermal areas derived from simplistic calculations without inclusion of heat-sink effect by the adjacent high-flow blood vessels (hepatic veins in this case). (b) Simulated isothermal areas after factoring in the flow of regional blood vessels (by adjusting the perfusion factor in the bioheat equation). Superimposing the thermal models on the respective axial CT images (c) and (d) predicts an area of suboptimal treatment (right inferior quadrant of the ablation zone along the medial aspect of the hepatic vein) and suggests the need for application of a balloon occlusion technique to temporarily arrest blood flow of the vein and minimize heat sink during thermal therapy. Reproduced with permission from Wood *et al.*, Journal of Vascular and Interventional Radiology **18**, 9–24 (2007). Copyright © 2007 Elsevier.

been described. Each temperature increase by 1 °C causes a decrease of tissue attenuation by 0.4 HU.[32,34] Z-axis coverage of last generation MDCT systems, combined with low-dose CT fluoroscopy settings, has the potential of near real-time calculation of tissue temperature changes during CT-guided tumor ablation, thereby facilitating the monitoring and control of treatment outcomes (Fig. 4).

II.D. Intravascular ultrasound and optical coherence tomography

Intravascular ultrasound (IVUS) and optical coherence tomography (OCT) are both catheter-based technologies used to produce high-resolution cross-sectional images of the vessel lumen and wall. In principle, IVUS is based on the emission,

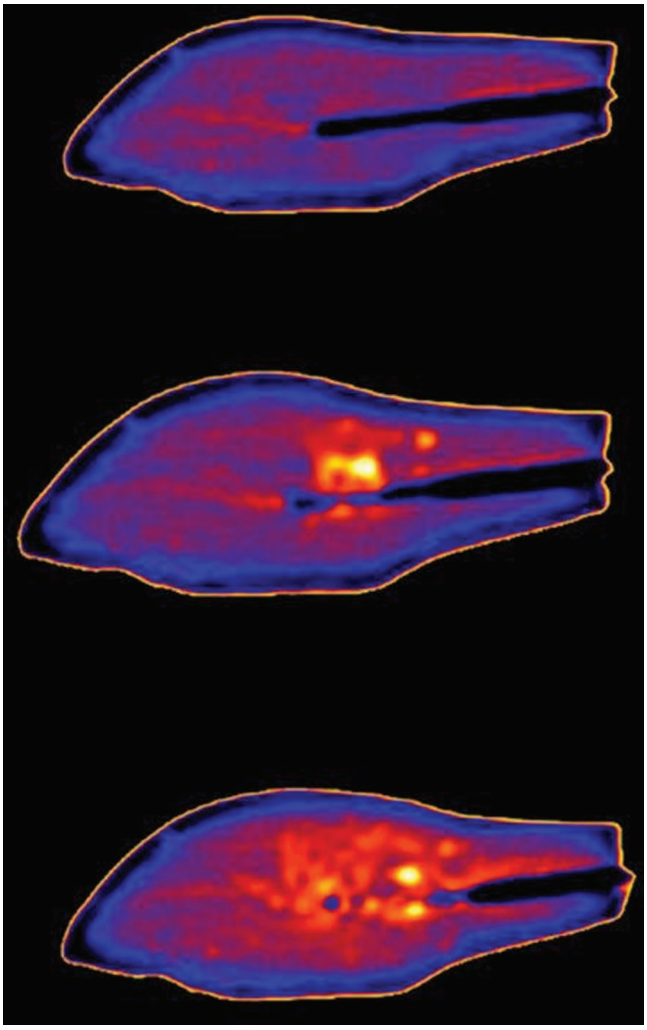

FIG. 4. Computed tomography thermometry. Grayscale CT images of liver specimen were obtained during heating with a bipolar RF probe. Increasing temperature is encoded by increasing brightness. At baseline (top) the temperature was 37 °C. The increase in temperature started close to the RF-probe (middle), and by convection the specimen was heated to 65 °C (bottom). Reproduced with permission by Mahnken *et al.*, International Journal of Clinical Practice Supplement **171**, 1–2 (2011). Copyright © 2011 Wiley.

attenuation, and backscattering of ultrasonic waves, whereas OCT is based on the emission and reflection of near-infrared light. In contrast to traditional angiography that identifies only the patent vessel lumen after injection of contrast agents, both IVUS and OCT can visualize structural details of atherosclerotic plaques, intimal dissections, and neointimal hyperplasia. In particular, OCT may provide highly detailed endoluminal pictures on a microscopic scale (10–100 μm resolution).[35] OCT datasets may be further postprocessed with automated software for robust quantification of the volume and extent of instent neointimal hyperplasia in the context of longitudinal studies evaluating the development of thrombus, stent malapposition, and strut endothelialization.[36] Vascular researchers may employ IVUS- or OCT-based measurements to derive key plaque features such as fibrous cap thickness and necrotic core volumetry, which may be further used as surrogate endpoints for the success of pharmacological interventions.[37–39] Most likely, IVUS and OCT could evolve from research tools to routine modalities of guidance during endovascular procedures. For example, several institutions already use intravascular imaging to evaluate balloon angioplasty outcomes and guide stent placement during coronary and peripheral angioplasty procedures.[35,40]

Image fusion of IVUS and/or OCT with digital angiography promises to offer enhanced image guidance during recanalization of complex lesions. Not only may it allow easier identification of high-risk lesions that may require use of peripheral embolic protection or direct stenting to minimize complications of peripheral thromboembolism but it may also provide the necessary guidance for precise tailoring of each treatment on an individual basis.[41] Eventually each step of an angioplasty procedure could be driven by a combination of imaging data depicting both the vessel lumen and the vessel wall so that complications are reduced, long-term outcomes are improved and services become more cost-effective. Researchers have already described a method for accurate coregistration of biplane x-ray angiography and IVUS/OCT cross-sectional images to produce a three-dimensional fused dataset of all modalities.[42] This approach provides superior guidance by extending imaging from plain angiography, which is actually just a lumenogram, to three-dimensional visualization that includes a wealth of vessel wall information. The operators can scroll through the segmented vessel centerline and analyze vessel lumen dimensions, the extent of the lesion, the exact plaque features, and the location of side-branches in detail.[42] Commercialization of user-friendly software tools for robust integration of IVUS/OCT acquisitions into real-time angiography, with additional incorporation of virtual histology algorithmic image analysis for enhanced operator perception of wall plaque anatomy and morphology, is expected to revolutionize the future of endovascular procedures. Nonetheless, application of such techniques may be limited to the coronary and peripheral arteries, since IVUS or OCT probes may be difficult to employ in anatomical territories with tortuous and/or small vessels such as the intracranial circulation.

Apart from conventional ultrasound and OCT, optical imaging technologies are anticipated to play an increasing role of image guidance in future IR applications. Human vision direction might be enhanced during image-guided procedures by various optical and optoacoustic (photoacoustic) techniques. Molecular optical imaging is already proving useful in the detection of fluoroscent or bioluminescent signals to improve the detection of malignant tissues. Narrow band spectral imaging, autofluorescence spectroscopy, and epi-illumination fluorescence imaging may augment the identification and characterization of superficial tissues during endoscopic procedures. Coupling of traditional x-ray guidance with highly sensitive optics may highlight subtle cancer lesions in deep-seated organs and assist in monitoring the kinetics and efficacy of systemically delivered target-specific therapeutic agents.[43,44] Photoacoustic imaging is a hybrid modality that uses light to produce ultrasonic waves for signal detection. Multispectral photoacoustic imaging combines tissue penetration of 0.5–2 cm with high spatial resolution of 30–200 μm, with the latter being inversely related to the

former. Interventional photoacoustic imaging may prove useful in the characterization of microvasculature hemodynamics and the kinetics of targeted optical-based probes such as gold nanorods and carbon nanotubes.[45] Integration of photoacoustic imaging probes in interventional instruments may improve minimally invasive procedures for the diagnosis and therapy of cancer.

II.E. Interventional MR and hybrid XMR

To date, x-ray angiography remains the method of choice for most routine transcatheter cardiovascular procedures. However, MR imaging has the advantage of combining high soft tissue contrast resolution with whole-body volume imaging without ionizing radiation.[46] Although dedicated interventional MR systems have been developed, most of today's MR-guided interventions are performed in utilitarian closed-bore magnets.[47] MR-compatible instrumentation is being developed for endovascular and cancer therapies. Commercially available low-strength (1.0 T) open-bore and high-strength (1.5 T) wide bore magnets are reshaping the field of interventional MR. C-shaped open-bore magnets allow increased patient access and are increasingly being used for biopsies, tumor ablation, and spine injections, although their low-strength vertical fields result in reduced signal-to-noise ratio (SNR) and low imaging speed.[48]

Interventional MR offers tremendous promise for IR procedures, because it is the only imaging modality with the potential to combine all four elements of IR guidance described previously. Real-time MR fluoroscopy sequences have been developed that permit identification of lesions not easily seen on CT or US, accurate tracking of interventional tools, and real-time physiologic monitoring of the delivered treatment.[48–51] MR may combine anatomic imaging with functional parameters such as blood flow, tissue oxygenation, and tissue temperature.[46] MR-perfusion and MR-thermometry may be performed during percutaneous tumor ablation to evaluate the extent of the necrosis and to document treatment outcomes.[28,52]

MR-guided high-intensity focused ultrasound (MRgHIFU) has been announced recently by several vendors and represents a unique combination of imaging and ablative technologies that provide noninvasive automated tissue thermoablation of the desired target.[53] HIFU is an innovative technique of thermoablation that does not require disruption of the skin barrier by scalpels or needles, but instead involves the transcutaneous delivery of focused beams of high-intensity ultrasound that produce coagulative necrosis of the targeted tissues. HIFU was introduced during the last decade for the noninvasive treatment of uterine, prostate, bone, and breast tumors, and MRI guidance has become the imaging mode of choice for delivery of real-time multiplanar guidance and physiologic thermometry monitoring during HIFU applications.[54,55] All necessary MRgHIFU functions are monitored and controlled remotely through a computer interface.[53,56–58] Apart from thermoablation, MR-guided focused ultrasound has been employed to enhance delivery and intratumoral uptake of chemotherapeutic agents in peripheral organs[56,59] or in the brain by producing localized and reversible disruption of the brain-blood barrier.[60,61]

MR-guided endovascular procedures are emerging and could have a major impact in cardiovascular care. Contrary to standard DSA lumenography, MR-angiography (MRA) can employ noncontrast or contrast-enhanced sequences and produce both two- and three-dimensional projections including the vessel wall. Arterial vessel wall imaging is critical in the assessment of atherosclerosis and may aid in endovascular therapies. Examples include evaluating vessel wall barotraumas and remodeling following balloon angioplasty, and monitoring the release of antirestenotic agents from the top surface of drug-eluting stents and drug-coated balloons.[62]

High SNR and imaging speed are necessary for real-time MR-fluoroscopic guided catheter steering and guidewire manipulation inside human vessels. Real-time imaging is available with steady-state free precession (SSFP) sequences, and diluted gadolinium agents may be infused to increase blood contrast and provide DSA-like angiography.[63] Intra-arterial injection of gadolinium remains an off-label use, but studies have shown the feasibility of injecting small aliquots of diluted gadolinium by the side-port of an arterial sheath similar to percutaneous angioplasty (Fig. 5).[64] Alternatively, newer blood pool contrast agents may be injected for steady state imaging with increased and prolonged contrast of the intravascular space.[46] Contrast-enhanced imaging, gradient imaging, and parallel acquisition techniques, including but not limited to SSFP, FIESTA, trueFISP, GRAPPA, and key hole, have been suggested for MR-guided endovascular procedures.[46] Future applications stand to

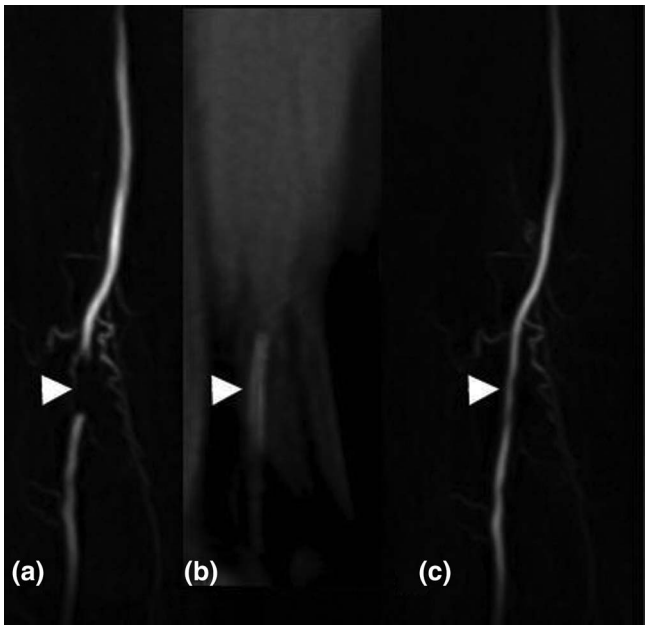

FIG. 5. MR-guided femoral balloon angioplasty. Intra-arterial MR angiography in a patient with peripheral arterial occlusive disease before (a), during (b), and after (c) dilatation of the femoral artery. Arrows show a short occlusion of the distal superficial femoral artery (a), the endovascular balloon-catheter in place (b), and the result after dilatation (c). Reproduced with permission by Kos *et al.*, European Radiology **18**, 645–657 (2008). Copyright © 2011 Springer.

gain a lot from novel accelerated time-resolved MRA acquisitions that produce four-dimensional vascular imaging datasets and may provide flexible roadmaps for interventional procedures.[65]

The main challenge in MR-guided procedures is the tracking of endovascular instruments. They may either be invisible if composed of plastic, or produce susceptibility artifacts if made of ferromagnetic alloys.[66] Passive and active methods have been proposed for real-time device tracking during interventional MR, but there are still substantive engineering hurdles to be overcome. Wires, catheters, and stents for routine MRI applications must be developed before use of MR-guided endovascular procedures can become routine. Development of MR-compatible 0.035-in. guidewires made from fiberglass or polyetheretherketone (PEEK) has been one of the more recent developments in this field.[66]

Hybrid XMR is the combination of real-time x-ray fluoroscopy with traditional MRI to guide catheters and needles with high spatial resolution and tissue anatomic detail.[67] XMR is a dual modality that combines the comfort and familiarity of x-ray fluoroscopy with the soft tissue detail and functional information provided by MRI. XMR procedures may involve fusion of datasets acquired at different time points, or near real-time combined x ray and MR fluoroscopic imaging by switching between the two modalities.[66,68] Different XMR engineering approaches have been pursued, with either the x-ray source positioned between two halves of the magnet, or the provision of two separate imaging systems in which the patient table can be railed from one to the other on a transport lane.[46] The challenge of hybrid XMR lies in overcoming the inherent incompatibilities between an x-ray source and a magnetic field. The electron beam inside the x-ray tube may be deflected or defocused by the magnetic field, and the electron beam inside the image intensifier is very sensitive to an external magnetic field.[69] Alternatively, an active magnetic shielding system that can correct for electron beam deflection and allow for placement and operation of the x-ray tube within close proximity (around 1 m) to the MRI scanner has been proposed.[70] With current technologies, though, simultaneous operation of the two systems remains impossible, and operators have to rely on techniques of image registration. Future applications of XMR may span angioplasty procedures, cardiac catheterizations, and targeted drug-delivery applications.[71]

II.F. Angiography and flat-panel CT

Today's x-ray imaging modalities are typically equipped with a rotating anode x-ray tube, and the emitted photons may be captured by traditional image intensifiers (IIs), modern CT detector arrays, or indirect or direct flat panel detectors (FPDs).[2,72] Even though CBCT with traditional IIs has been reported for almost a decade,[73] introduction of FPDs into the interventional suite has allowed CBCT applications with enhanced image quality and larger fields of view. FPDs are of special interest to radiological interventions because of their combined planar and tomographic imaging capability. FPDs have higher instrumentation noise and limited dynamic imaging properties compared with phosphor-based image intensifiers, but their advantages include smaller physical dimensions, reduced distortion, and CBCT applications.[74] FPD-based CBCT has improved spatial and soft-tissue resolution compared with II-based CBCT.

Digital flat panel angiography units offer a combination of real-time fluoroscopic and near real-time tomographic imaging of the anatomy of interest.[75–77] Such two-in-one hybrid image-guidance offers advantages because the interventionalist may combine high resolution cross-sectional CBCT morphological information with the expediency of standard angiography.[78,79] Furthermore, mobile C-arms with 3D-imaging capabilities have been designed for the hybrid operating theaters of the future. Examples include the O-arm (Medtronic),[80,81] Vision Vario 3D (Ziehm Imaging), and other prototypes.[82–84] Although those systems have been designed for intraoperative cross-sectional imaging during spine and orthopedic surgery, they provide a further proof of concept for combined fluoroscopic and volumetric imaging and may become part of state-of-the art hybrid interventional suites of the future. These imaging systems also have a more compact design and might result in significant space and cost savings.

Of special interest, C-arm CBCT may soon offer the capacity for performing noncircular scanning trajectories. Typically, the x-ray source and the II or FPD rotate in a circle around the body. However, circular acquisitions may yield insufficient body coverage. Methods for performing noncircular scan geometries have been proposed and in the future a combination of trajectories with nonisocentric orbits may be available for organ-specific CBCT imaging.[85,86] Incorporation of novel high-sensitivity microangiographic detectors, or alternatively solid-state image intensifiers, might further increase resolution, lower noise, and improve dynamic imaging of FPD x-ray units.[87–89]

Image fusion software applications that superimpose cross-sectional CBCT datasets or three-dimensional rotational angiography onto real-time fluoroscopy are already commercially available from several vendors. In this manner, hybrid flat panel units offer virtual three-dimensional roadmapping capability during delicate brain endovascular procedures such as embolization of cerebral aneurysms or malformations (Fig. 6).[90] Exquisite anatomical detail combined with three-dimensional presentation of the angioarchitecture enhances operator cognition and increases procedural success and safety by limiting the risk of inadvertent nontarget embolization. Hemodynamic characterization of the target vessels with on-demand CFD algorithms, and fusion of relevant CFD maps with traditional angiograms, could provide more robust assessment of vascular disease and further enhance the operator's experience and confidence during performance of complex endovascular procedures.[91]

III. EMERGING DEVICE NAVIGATION AND TRACKING TECHNOLOGIES

III.A. Optical and electromagnetic tracking

Device tracking and navigation developments may be needle-based, catheter-based, or image-based. Integration of

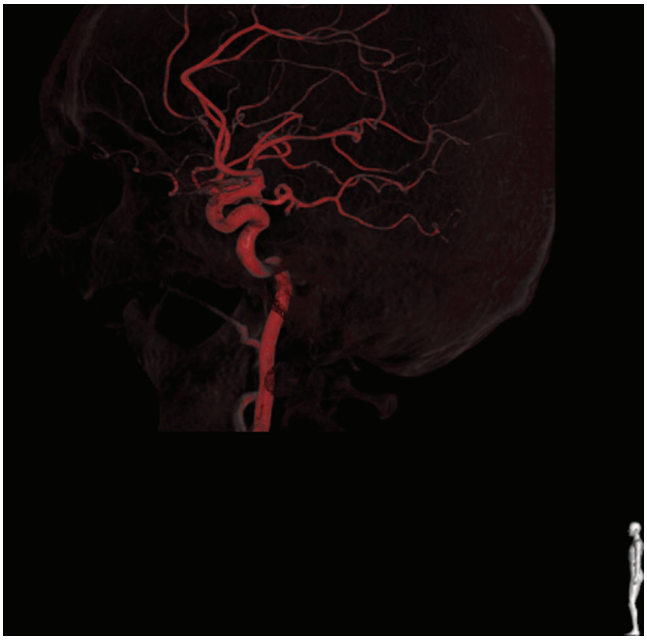

FIG. 6. Contrast-enhanced cone-beam CT cerebral angiogram with a flat panel angiography unit. A three-dimensional volume-rendered image of the cerebral vasculature is reconstructed that may be fused with intraprocedural x-ray fluoroscopy to serve as a 3D roadmap during wire navigation (XperCT – 3D RoadMap, Philips, Germany). As the c-arm rotates around the head, the 3D roadmap rotates accordingly to match the image.

position sensors with interventional tools such as ultrasound transducers, angiography catheters, stents, biopsy needles, and ablation electrodes permits real-time tracking of the position of the tools in a three-dimensional Cartesian coordinate system.[92] Device position tracking is enabled by appropriate sensors integrated with the medical devices, and location information is recorded by optical or infrared cameras, or by a small electromagnetic field generator. Optical tracking incorporates reflective passive markers or active light emission and requires a direct line of sight to be successful. Electromagnetic tracking uses small coils integrated with the medical devices to be able to pinpoint their exact location within space. A new form of electromagnetic tracker based on window field generation that may be better suited to fluoroscopy and cone-beam CT has been recently reported.[93]

EM tracking of interventional devices may use real-time US guidance and fusion with preprocedural CT images to perform an IR procedure without any intraprocedural radiation but with very accurate targeting. Contrary to optical tracking, EM tracking is effective in tracking flexible instruments such as catheters and wires.[94] Electromagnetic navigation of interventional tools is described as equivalent to a miniaturized medical GPS for tracking the position of instruments inside the human body.[6,92] However, EM tracking is operational only within a small field of view and suffers from artifacts produced by large metal objects that may distort the electromagnetic field. During tracking, the position of the sensor, corresponding, for example, to the tip of a catheter or a needle, may be displayed on x-ray or US images, or may be projected on more complex fused images (e.g., CT/US or XMR). Therefore, navigation technologies have to contend with the same image registration challenges and hurdles as those encountered with image fusion technologies.[6,94,95] Prototype software applications try to combine multimodality image registration and fusion with electromagnetic tracking and robotic guidance in a seamless, "see-and-treat" environment.[6] Modern device tracking and navigation in IR is merging with high-tech computerized interfaces similar to video games.[92] At the moment, some vendors are producing commercial versions of EM tracking solutions with up to 6 degrees of freedom (DOF), and the technology is increasingly being adopted by IR physicians along with multimodality, usually CT/US, image registration. EM tracking has been shown to improve targeting accuracy during tumor biopsy and ablation, and further advantages in terms of augmented pretreatment planning have been postulated.[96] It has also been tested in various experimental image-guided IR procedures such as liver radiofrequency ablation, transjugular intrahepatic portosystemic shunts, vertebroplasty, and carotid stent placement.[94,97] Target registration error (TRE) has been reported to be in the range of a few millimeters for both optical and electromagnetic approaches,[96,98,99] with optical methods being slightly more accurate than EM tracking.[100]

III.B. Remote device actuation

Guidewires used in routine interventions are basically passive tubes made of metal alloys or synthetic polymers. Guidewires are inserted and maneuvered under x-ray guidance inside vessels and hollow organs with direct human interaction, with the operator pushing, pulling, or rotating the guidewire in conjunction with a catheter that helps to orient and guide advancement of the wire to the desired destination. There has been a surge of technologies aiming to convert the passive nature of guidewire-steered device manipulation into more active device navigation. Shape memory alloys, microengineering, and microelectronics have raised the sophistication of interventional needles, catheters, wires, probes, and electrodes.[101] Investigators are exploring several avenues toward improving the feasibility and accuracy of targeting difficult or sometimes even impossible-to-reach anatomical targets. Steerable bevel-tip needles that may bypass sensitive structures by following curved pathways,[102] steerable endovascular catheters that navigate inside the heart chambers,[103,104] or even snake-arm or elephant-trunk robotic arms[105] may someday be used routinely in image-guided interventions to gain access to very distal and tortuous vessels.

Remote device actuation is becoming a reality with the introduction of novel magnetic-field enabled instruments and remote robotic steering systems.[106,107] Both of these technological trends have the potential to transform the entire landscape of interventional radiology. Magnetic fields were first used more than 50 yr ago to guide a steel-tip catheter in the rabbit aorta.[108] Over the last decade, magnetic navigation has made phenomenal leaps forward and presently offers endovascular navigation of a guidewire with high precision. Quite simply, magnetic navigation promises

superior guidewire steerage and maneuverability by employing external magnetic fields that can navigate the tip of a magnetically enabled catheter in the desired direction.[109] It offers omnidirectional guidewire manipulation with great potential for treatment of chronic total occlusions (CTO) and lesions located in hostile or difficult-to-reach anatomic regions.[109] Currently, the NIOBE Magnetic Navigation system (Stereotaxis, St.Louis, MO, US) and the CGCI system (Magnetecs, Inglewood, CA, US) have been licensed for transcatheter endovascular procedures. In both systems, a sophisticated computer interface allows the operator to remotely navigate inside the cardiac chambers and track tortuous vascular anatomies using joystick handles and other haptics with real-time feedback. Briefly, the Stereotaxis system involves two permanent external magnets, with one on each side of the body, that produce a low-strength magnetic field (0.08 T). Computer-guided mechanical movement of the external magnets changes the orientation of the magnetic fields of the magnets. This causes realignment of a magnet-tipped catheter to become parallel to the orientation of the new composite magnetic field, while a computer-controlled system advances the catheter.[110,111] In the Magnetecs system, eight external electromagnets are positioned semispherically around the human chest to produce a lobe-shaped, dynamic, 0.14 T magnetic field. Rapid changes in the magnitude, direction, and gradient of the magnetic field produce a nearly real-time pull/push and torque/bend motion of the tip of a proprietary magnet-tipped catheter.[112] Magnetic navigation systems may fuse image datasets from MDCT or MRI with x-ray fluoroscopy to provide intuitive three-dimensional images with a stereotactic presentation during endovascular catheter procedures.[113–115]

In principle, external permanent magnets produce a low-strength uniform magnetic field of about 15 cm in diameter that can be freely directed within a region of interest after the patient has been properly placed and isocentered. Within this spherical magnetic field, magnetic vectors are applied to achieve 360° rotation of a wire or catheter carrying a 2–3 mm tip-mounted magnet. Clinical applications encompass steerable angioplasty guidewires and cardiac electrophysiology ablation catheters, radiofrequency-enabled guidewires that can cross tight total occlusions, multidirectional endovascular probes, and directional needle-tip catheters for targeted cardiac stem cell transplantation.[109] Phantom studies with the Stereotaxis system have demonstrated accurate and fast navigation inside models of human cerebral and celiac hepatic arteries.[116,117] Magnetic-assisted navigation has been described as the primary or secondary (after failed manual technique) mode of guidance for percutaneous coronary interventions.[118,119] Its utility has been also explored in the recanalization of coronary CTOs, where the system may overlay an image of the vessel isocentral axis by incorporating IVUS, OCT, or MDCT angiographic datasets. In this way, the operator may "look forward" inside the occlusion as the guidewire advances so as to avoid vessel rupture or perforation.[109] An analysis of 350 consecutive coronary interventions performed with the Stereotaxis Niobe magnetic navigation system reported a 93% success rate to cross the lesion with the magnetically enabled guidewire without any perforations or dissections. Nonetheless, the learning curve was steep and more than 80 cases were necessary to reach a plateau of adequate experience with the system.[120]

III.C. Interventional robotics

Following developments in surgical laparoscopy and other fields of medicine, interventional robots capable of performing CT-, MR-, US-, or x-ray guided procedures have been developed.[121–123] Robots are not designed to replace humans but to augment the physician by imparting superhuman capabilities. Interventional robots offer several degrees of freedom and superior accuracy, stability, and dexterity during device navigation, propulsion, and actuation.[122,124,125] IR robots may receive guidance input by single modality imaging or fused multimodality imaging. For example, a CT-integrated robot (NIH, Bethesda, MD and Philips Medical Systems) has been developed that is able to complete all steps of image capture, registration, and fusion, and to insert a needle into the human body with semiautonomous or completely autonomous operations.[126] Another prototype robot that is placed on top of the patient's body (patient-mounted) may be either CT- or MR-compatible and has multiple degrees of freedom (5 DOF) during device actuation.[127,128] Design and engineering of MR-compatible robots is challenging because ordinary electric motors and other ferromagnetic materials typically used in engineering may interfere with the magnetic field and the RF imaging pulses. Hence, construction of MR-compatible robots must employ nonmetal structures and piezoelectric, pneumatic, or hydraulic motor systems.[123,125] TRE of a robotic CT-guided navigation system for needle placement has been reported to be about 1 mm.[122]

In the endovascular arena, the limited flexibility, trackability, and maneuverability of endovascular tools has motivated the development of catheters that are steered and controlled remotely by specially designed robotic arms. It has been postulated that remote robotic catheter navigation may achieve more stable and precise catheter negotiation within the arterial tree, thereby decreasing the risk of vessel trauma or nontarget embolization, which could have serious consequences such as brain stroke in case of emboli dislodged from the aortic arch and the great vessels during catheter manipulation.[129,130] The Magellan Robotic system (Hansen Medical, Mountain View, California) is a "master-slave" system that enables the physician to control and advance steerable catheters remotely within large arteries. The physician is situated at a remote workstation away from the patient and from the radiation field. The physician controls a three-dimensional mouse with tactile feedback, and the control workstation uses electromechanics to translate the human haptic orders into accurate movements of the tip of a guide catheter and sheath with seven degrees of freedom. The workstation may display preoperative CT images, x-ray fluoroscopy, and a cartesian 3D representation of the location of the catheter tip. This system has been applied successfully for arch vessel cannulation and for deployment of abdominal aortic stent-grafts.[131–133] The

technology is still limited by the large size of the robotic sheath (11-14 Fr) and is therefore not applicable in more demanding, small, tortuous visceral, and cerebral arteries. The system may prove particularly useful in achieving *in situ* fenestration of aortic stents, which would obviate the need for expensive, customized stents that are expensive and time-consuming to produce.[131] There is also the potential that the joystick-control platforms used in most of today's robotic control systems will be replaced by 3D scanning devices and depth cameras (i.e., Microsoft Kinect systems) that are able to track and identify body motion in real-time and provide augmented touch-free interaction between humans and machines.[134]

IV. CONCLUSION

By 2020, most of the image guidance pillars described in this article might merge into autonomous, multimodality, multiparametric platforms that offer real-time data on anatomy, morphology, function, and metabolism along with real-time computational modeling and robotic navigation and actuation of interventional instruments (Fig. 7). Optimization of tracking and navigation of interventional tools inside the human body will be critical in converting IR suites into the minimally invasive operating theaters of the future with increased safety and unsurpassed therapeutic efficacy. Navigation systems could be fully integrated into imaging systems by being embedded in the theater table or CT gantry. Hybrid XMR systems that deliver simultaneous x-ray and MR real-time imaging probably lie in the more distant future, whereas solely MR-guided IR could become a field of its own. Remote magnetic-enabled catheter manipulation may increase in sophistication, precision, and degrees of freedom as higher-strength and localized magnetic fields are developed. Interventional robots could continue to develop and transform IR practice by minimizing personnel radiation exposure and augmenting minimally invasive therapies with more accurate and dexterous tool handling than can be achieved by humans alone. Remote performance of IR procedures via teleoperation of IR robots could become a new frontier for telemedicine and telesurgery that will deliver high-quality services to remote or inhospitable places on earth or even during deep space exploration missions. Technological developments in image guidance and device navigation will continue to drive a very bright future for interventional radiology and image-guided medicine in general.

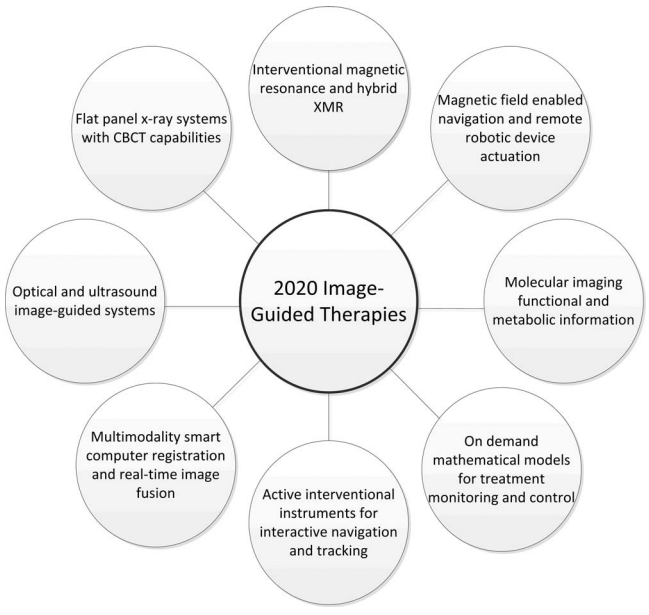

FIG. 7. The pillars of 2020 image-guidance and device navigation technologies. The authors envision that by 2020 most of the image guidance pillars described herein might merge into autonomous, multimodality, multiparametric platforms that will offer real-time data on anatomy, morphology, function, metabolism along with real-time computational modeling and robotic navigation and actuation of interventional instruments.

ACKNOWLEDGMENT

This research has been co-financed by the European Union (European Social Fund—ESF) and Greek national funds through the Joint Research and Technology Program between Greece and France (2009–2011).

[a]Author to whom correspondence should be addressed. Electronic mail: gkagad@gmail.com and George.Kagadis@med.upatras.gr; Telephone: +30 2610 969146; Fax: +30 2610 969166.

[1]S. B. Solomon and S. G. Silverman, "Imaging in interventional oncology," Radiology **257**, 624–640 (2010).
[2]S. Rudin, D. R. Bednarek, and K. R. Hoffmann, "Endovascular image-guided interventions (EIGIs)," Med. Phys. **35**, 301–309 (2008).
[3]P. Haigron, J. L. Dillenseger, L. Luo, and J. L. Coatrieux, "Image-guided therapy: Evolution and breakthrough," IEEE Eng. Med. Biol. Mag. **29**, 100–104 (2010).
[4]G. C. Kagadis, K. K. Delibasis, G. K. Matsopoulos, N. A. Mouravliansky, P. A. Asvestas, and G. C. Nikiforidis, "A comparative study of surface- and volume-based techniques for the automatic registration between CT and SPECT brain images," Med. Phys. **29**, 201–213 (2002).
[5]P. A. van den Elsen, E.-J. D. Pol, and M. A. Viergever, "Medical image matching: A review with classification," IEEE Eng. Med. Biol. **12**, 26–39 (1993).
[6]B. J. Wood *et al.*, "Technologies for guidance of radiofrequency ablation in the multimodality interventional suite of the future," J. Vasc. Interv. Radiol. **18**, 9–24 (2007).
[7]B. Glocker, A. Sotiras, N. Komodakis, and N. Paragios, "Deformable medical image registration: Setting the state of the art with discrete methods," Annu. Rev. Biomed. Eng. **13**, 219–244 (2011).
[8]E. C. Ford, J. Herman, E. Yorke, and R. L. Wahl, "18F-FDG PET/CT for image-guided and intensity-modulated radiotherapy," J. Nucl. Med. **50**, 1655–1665 (2009).
[9]J. T. Yap, J. P. Carney, N. C. Hall, and D. W. Townsend, "Image-guided cancer therapy using PET/CT," Cancer J. **10**, 221–233 (2004).
[10]A. M. Avram, "Radioiodine scintigraphy with SPECT/CT: An important diagnostic tool for thyroid cancer staging and risk stratification," J. Nucl. Med. **53**, 754–764 (2012).
[11]H. Zaidi and A. Del Guerra, "An outlook on future design of hybrid PET/MRI systems," Med. Phys. **38**, 5667–5689 (2011).
[12]G. C. Kagadis, G. Loudos, K. Katsanos, S. G. Langer, and G. C. Nikiforidis, "In vivo small animal imaging: Current status and future prospects," Med. Phys. **37**, 6421–6442 (2010).
[13]D. A. Torigian, S. S. Huang, M. Houseni, and A. Alavi, "Functional imaging of cancer with emphasis on molecular techniques," Ca-Cancer J. Clin. **57**, 206–224 (2007).
[14]A. M. Venkatesan *et al.*, "Real-time FDG PET guidance during biopsies and radiofrequency ablation using multimodality fusion with electromagnetic navigation," Radiology **260**, 848–856 (2011).

[15]C. Karmonik, J. X. Bismuth, M. G. Davies, and A. B. Lumsden, "Computational hemodynamics in the human aorta: A computational fluid dynamics study of three cases with patient-specific geometries and inflow rates," Technol. Health Care **16**, 343–354 (2008).
[16]C. Canstein *et al.*, "3D MR flow analysis in realistic rapid-prototyping model systems of the thoracic aorta: Comparison with in vivo data and computational fluid dynamics in identical vessel geometries," Magn. Reson. Med. **59**, 535–546 (2008).
[17]Y. S. Khajanchee, D. Streeter, L. L. Swanstrom, and P. D. Hansen, "A mathematical model for preoperative planning of radiofrequency ablation of hepatic tumors," Surg. Endosc. **18**, 696–701 (2004).
[18]C. Villard, C. Baegert, P. Schreck, L. Soler, and A. Gangi, "Optimal trajectories computation within regions of interest for hepatic RFA planning," Med. Image Comput. Comput. Assist. Interv. **8**, 49–56 (2005).
[19]C. Villard, L. Soler, and A. Gangi, "Radiofrequency ablation of hepatic tumors: Simulation, planning, and contribution of virtual reality and haptics," Comput. Methods Biomech. Biomed. Engin. **8**, 215–227 (2005).
[20]A. Erhart, E. Divo, and A. Kassab, "An evolutionary-based inverse approach for the identification of non-linear heat generation rates in living tissues using a localized meshless method," Int. J. Numer. Methods Heat Fluid Flow **18**, 401–414 (2008).
[21]L. Assumpcao, M. Choti, T. M. Pawlik, J. F. Gecshwind, and I. R. Kamel, "Functional MR imaging as a new paradigm for image guidance," Abdom. Imaging **34**, 675–685 (2009).
[22]D. Yudovsky, A. Nouvong, K. Schomacker, and L. Pilon, "Assessing diabetic foot ulcer development risk with hyperspectral tissue oximetry," J. Biomed. Opt. **16**, 026009 (2011).
[23]D. Yudovsky, A. Nouvong, and L. Pilon, "Hyperspectral imaging in diabetic foot wound care," J. Diabetes Sci. Technol. **4**, 1099–1113 (2010).
[24]I. Eitel *et al.*, "Long-term prognostic value of myocardial salvage assessed by cardiovascular magnetic resonance in acute reperfused myocardial infarction," Heart **97**, 2038–2045 (2011).
[25]C. H. Thng, T. S. Koh, D. J. Collins, and D. M. Koh, "Perfusion magnetic resonance imaging of the liver," World J. Gastroenterol. **16**, 1598–1609 (2010).
[26]A. Boss *et al.*, "Morphological, contrast-enhanced and spin labeling perfusion imaging for monitoring of relapse after RF ablation of renal cell carcinomas," Eur. Radiol. **16**, 1226–1236 (2006).
[27]R. Puls *et al.*, "Laser ablation of liver metastases from colorectal cancer with MR thermometry: 5-year survival," J. Vasc. Interv. Radiol. **20**, 225–234 (2009).
[28]B. D. de Senneville, C. Mougenot, B. Quesson, I. Dragonu, N. Grenier, and C. T. Moonen, "MR thermometry for monitoring tumor ablation," Eur. Radiol. **17**, 2401–2410 (2007).
[29]M. S. Breen, M. Breen, K. Butts, L. Chen, G. M. Saidel, and D. L. Wilson, "MRI-guided thermal ablation therapy: Model and parameter estimates to predict cell death from MR thermometry images," Ann. Biomed. Eng. **35**, 1391–1403 (2007).
[30]B. Quesson, J. A. de Zwart, and C. T. Moonen, "Magnetic resonance temperature imaging for guidance of thermotherapy," J. Magn. Reson. Imaging **12**, 525–533 (2000).
[31]T. Sabharwal, K. Katsanos, X. Buy, and A. Gangi, "Image-guided ablation therapy of bone tumors," Semin Ultrasound CT MR **30**, 78–90 (2009).
[32]A. H. Mahnken and P. Bruners, "CT thermometry: Will it ever become ready for use?," Int. J. Clin. Pract. Suppl. **65**(S171), 1–2 (2011).
[33]R. M. Arthur, W. L. Straube, J. W. Trobaugh, and E. G. Moros, "Noninvasive estimation of hyperthermia temperatures with ultrasound," Int. J. Hyperthermia **21**, 589–600 (2005).
[34]B. G. Fallone, P. R. Moran, and E. B. Podgorsak, "Noninvasive thermometry with a clinical x-ray CT scanner," Med. Phys. **9**, 715–721 (1982).
[35]D. Karnabatidis, K. Katsanos, I. Paraskevopoulos, A. Diamantopoulos, S. Spiliopoulos, and D. Siablis, "Frequency-domain intravascular optical coherence tomography of the femoropopliteal artery," Cardiovasc. Intervent Radiol. **34**, 1172–1181 (2011).
[36]S. Tsantis, G. C. Kagadis, K. Katsanos, D. Karnabatidis, G. Bourantas, and G. C. Nikiforidis, "Automatic vessel lumen segmentation and stent strut detection in intravascular optical coherence tomography," Med. Phys. **39**, 503–513 (2012).
[37]C. A. Van Mieghem *et al.*, "Noninvasive detection of subclinical coronary atherosclerosis coupled with assessment of changes in plaque characteristics using novel invasive imaging modalities: The Integrated Biomarker and Imaging Study (IBIS)," J. Am. Coll. Cardiol. **47**, 1134–1142 (2006).
[38]M. Sonka, R. W. Downe, J. W. Garvin, J. Lopez, T. Kovarnik, and A. Wahle, "IVUS-based assessment of 3D morphology and virtual histology: Prediction of atherosclerotic plaque status and changes," Conf. Proc. IEEE Eng. Med. Biol. Soc. **2011**, 6647–6650 (2011).
[39]L. Inglese, C. Fantoni, and V. Sardana, "Can IVUS-virtual histology improve outcomes of percutaneous carotid treatment?," J. Cardiovasc. Surg. (Torino) **50**, 735–744 (2009).
[40]H. G. Bezerra, M. A. Costa, G. Guagliumi, A. M. Rollins, and D. I. Simon, "Intracoronary optical coherence tomography: A comprehensive review clinical and research applications," JACC Cardiovasc. Interv. **2**, 1035–1046 (2009).
[41]R. Puri, M. I. Worthley, and S. J. Nicholls, "Intravascular imaging of vulnerable coronary plaque: Current and future concepts," Nat. Rev. Cardiol. **8**, 131–139 (2011).
[42]S. Tu, N. R. Holm, G. Koning, Z. Huang, and J. H. Reiber, "Fusion of 3D QCA and IVUS/OCT," Int. J. Cardiovasc. Imaging **27**, 197–207 (2011).
[43]A. Bunschoten *et al.*, "Multimodal interventional molecular imaging of tumor margins and distant metastases by targeting alphavbeta3 integrin," ChemBioChem **13**, 1039–1045 (2012).
[44]X. Yang, "Interventional molecular imaging," Radiology **254**, 651–654 (2010).
[45]A. Sarantopoulos, N. Beziere, and V. Ntziachristos, "Optical and optoacoustic interventional imaging," Ann. Biomed. Eng. **40**, 346–366 (2012).
[46]S. Kos, R. Huegli, G. M. Bongartz, A. L. Jacob, and D. Bilecen, "MR-guided endovascular interventions: A comprehensive review on techniques and applications," Eur. Radiol. **18**, 645–657 (2008).
[47]S. Tatli, P. R. Morrison, K. Tuncali, and S. G. Silverman, "Interventional MRI for oncologic applications," Tech. Vasc. Interv. Radiol. **10**, 159–170 (2007).
[48]S. G. Silverman, K. Tuncali, and P. R. Morrison, "MR Imaging-guided percutaneous tumor ablation," Acad. Radiol. **12**, 1100–1109 (2005).
[49]S. R. Yutzy and J. L. Duerk, "Pulse sequences and system interfaces for interventional and real-time MRI," J. Magn. Reson. Imaging **27**, 267–275 (2008).
[50]H. Saybasili, A. Z. Faranesh, C. E. Saikus, C. Ozturk, R. J. Lederman, and M. A. Guttman, "Interventional MRI using multiple 3D angiography roadmaps with real-time imaging," J. Magn. Reson. Imaging **31**, 1015–1019 (2010).
[51]S. G. Silverman *et al.*, "Renal tumors: MR imaging-guided percutaneous cryotherapy–initial experience in 23 patients," Radiology **236**, 716–724 (2005).
[52]S. Roujol, M. Ries, B. Quesson, C. Moonen, and B. Denis de Senneville, "Real-time MR-thermometry and dosimetry for interventional guidance on abdominal organs," Magn. Reson. Med. **63**, 1080–1087 (2010).
[53]X. Meng *et al.*, "A comparative study of fibroid ablation rates using radio frequency or high-intensity focused ultrasound," Cardiovasc. Intervent Radiol. **33**, 794–799 (2010).
[54]T. Yu and J. Luo, "Adverse events of extracorporeal ultrasound-guided high intensity focused ultrasound therapy," PLoS ONE **6**, e26110 (2011).
[55]F. Orsi, P. Arnone, W. Chen, and L. Zhang, "High intensity focused ultrasound ablation: A new therapeutic option for solid tumors," J. Cancer Res. Ther. **6**, 414–420 (2010).
[56]Z. Mu, C. M. Ma, X. Chen, D. Cvetkovic, A. Pollack, and L. Chen, "MR-guided pulsed high intensity focused ultrasound enhancement of docetaxel combined with radiotherapy for prostate cancer treatment," Phys. Med. Biol. **57**, 535–545 (2012).
[57]D. W. Stovall, "Alternatives to hysterectomy: Focus on global endometrial ablation, uterine fibroid embolization, and magnetic resonance-guided focused ultrasound," Menopause **18**, 437–444 (2011).
[58]M. O. Kohler *et al.*, "Volumetric HIFU ablation under 3D guidance of rapid MRI thermometry," Med. Phys. **36**, 3521–3535 (2009).
[59]L. Chen, Z. Mu, P. Hachem, C. M. Ma, A. Wallentine, and A. Pollack, "MR-guided focused ultrasound: Enhancement of intratumoral uptake of [(3)H]-docetaxel in vivo," Phys. Med. Biol. **55**, 7399–7410 (2010).
[60]C. Y. Ting *et al.*, "Concurrent blood-brain barrier opening and local drug delivery using drug-carrying microbubbles and focused ultrasound for brain glioma treatment," Biomaterials **33**, 704–712 (2012).
[61]M. Kinoshita, "Targeted drug delivery to the brain using focused ultrasound," Top. Magn. Reson. Imaging **17**, 209–215 (2006).
[62]R. Wyttenbach *et al.*, "Effects of percutaneous transluminal angioplasty and endovascular brachytherapy on vascular remodeling of human femoropopliteal artery: 2 years follow-up by noninvasive magnetic resonance imaging," Eur. J. Vasc. Endovasc. Surg. **34**, 416–423 (2007).

[63]R. W. Huegli, M. Aschwanden, K. Scheffler, and D. Bilecen, "Fluoroscopic contrast-enhanced MR angiography with a magnetization-prepared steady-state free precession technique in peripheral arterial occlusive disease," AJR, Am. J. Roentgenol. **187**, 242–247 (2006).
[64]S. Potthast, A. C. Schulte, G. M. Bongartz, R. Hugli, M. Aschwanden, and D. Bilecen, "Low-dose intra-arterial contrast-enhanced MR aortography in patients based on a theoretically derived injection protocol," Eur. Radiol. **15**, 2347–2353 (2005).
[65]C. A. Mistretta, "Sub-Nyquist acquisition and constrained reconstruction in time resolved angiography," Med. Phys. **38**, 2975–2985 (2011).
[66]S. Kos *et al.*, "MR-compatible polyetheretherketone-based guide wire assisting MR-guided stenting of iliac and supraaortic arteries in swine: Feasibility study," Minimally Invasive Ther. Allied Technol. **18**, 181–188 (2009).
[67]L. F. Gutierrez *et al.*, "Technology preview: X-ray fused with magnetic resonance during invasive cardiovascular procedures," Catheter Cardiovasc. Interv. **70**, 773–782 (2007).
[68]R. Razavi *et al.*, "Cardiac catheterisation guided by MRI in children and adults with congenital heart disease," Lancet **362**, 1877–1882 (2003).
[69]R. Fahrig *et al.*, "A truly hybrid interventional MR/X-ray system: Feasibility demonstration," J. Magn. Reson. Imaging **13**, 294–300 (2001).
[70]J. A. Bracken, G. DeCrescenzo, P. Komljenovic, P. V. Lillaney, R. Fahrig, and J. A. Rowlands, "Closed bore XMR (CBXMR) systems for aortic valve replacement: Active magnetic shielding of x-ray tubes," Med. Phys. **36**, 1717–1726 (2009).
[71]A. Arepally, "Targeted drug delivery under MRI guidance," J. Magn. Reson. Imaging **27**, 292–298 (2008).
[72]M. J. Eagleton, "Intraprocedural imaging: Flat panel detectors, rotational angiography, FluoroCT, IVUS, or still the portable C-arm?," J. Vasc. Surg. **52**, 50S–59S (2010).
[73]U. Linsenmaier *et al.*, "Three-dimensional CT with a modified C-arm image intensifier: Feasibility," Radiology **224**, 286–292 (2002).
[74]D. J. Tward and J. H. Siewerdsen, "Cascaded systems analysis of the 3D noise transfer characteristics of flat-panel cone-beam CT," Med. Phys. **35**, 5510–5529 (2008).
[75]E. Liapi, K. Hong, C. S. Georgiades, and J. F. Geschwind, "Three-dimensional rotational angiography: Introduction of an adjunctive tool for successful transarterial chemoembolization," J. Vasc. Interv. Radiol. **16**, 1241–1245 (2005).
[76]A. L. Tam *et al.*, "C-arm cone beam computed tomography needle path overlay for fluoroscopic guided vertebroplasty," Spine **35**, 1095–1099 (2010).
[77]M. J. Wallace, "C-arm computed tomography for guiding hepatic vascular interventions," Tech. Vasc. Interv. Radiol. **10**, 79–86 (2007).
[78]S. Kakeda *et al.*, "Usefulness of cone-beam volume CT with flat panel detectors in conjunction with catheter angiography for transcatheter arterial embolization," J. Vasc. Interv. Radiol. **18**, 1508–1516 (2007).
[79]S. Hirota *et al.*, "Cone-beam CT with flat-panel-detector digital angiography system: Early experience in abdominal interventional procedures," Cardiovasc. Intervent Radiol. **29**, 1034–1038 (2006).
[80]F. Schils, "O-arm-guided balloon kyphoplasty: Prospective single-center case series of 54 consecutive patients," Neurosurgery **68**, 250–256 (2011).
[81]F. Caire, C. Gantois, F. Torny, D. Ranoux, A. Maubon, and J. J. Moreau, "Intraoperative use of the Medtronic O-arm for deep brain stimulation procedures," Stereotact. Funct. Neurosurg. **88**, 109–114 (2010).
[82]E. King *et al.*, "Intraoperative cone-beam CT for head and neck surgery: Feasibility of clinical implementation using a prototype mobile C-arm," Head Neck (to be published).
[83]S. Schafer *et al.*, "Mobile C-arm cone-beam CT for guidance of spine surgery: Image quality, radiation dose, and integration with interventional guidance," Med. Phys. **38**, 4563–4574 (2011).
[84]J. H. Siewerdsen *et al.*, "Volume CT with a flat-panel detector on a mobile, isocentric C-arm: Pre-clinical investigation in guidance of minimally invasive surgery," Med. Phys. **32**, 241–254 (2005).
[85]C. Seungryong, C. A. Pelizzari, and P. Xiaochuan, "Non-circular cone beam CT trajectories: A preliminary investigation on a clinical scanner," *Nuclear Science Symposium Conference Record (NSS/MIC)* (IEEE, 2000), pp. 3172–3175.
[86]D. Xia, S. Cho, and X. Pan, "Image reconstruction in reduced circular sinusoidal cone-beam CT," J. X-Ray Sci. Technol. **17**, 189–205 (2009).
[87]G. K. Yadava, S. Rudin, A. T. Kuhls-Gilcrist, and D. R. Bednarek, "Generalized objective performance assessment of a new high-sensitivity microangiographic fluoroscopic (HSMAF) imaging system," Proc. Soc. Photo–Opt. Instrum. Eng. **6913**, 69130U (2008).
[88]A. Kuhls-Gilcrist, G. Yadava, V. Patel, A. Jain, D. R. Bednarek, and S. Rudin, "The solid-state x-ray image intensifier (SSXII): An EMCCD-based x-ray detector," Proc. Soc. Photo–Opt. Instrum. Eng. **6913**, 69130K (2008).
[89]P. Sharma *et al.*, "EMCCD-based high resolution dynamic x-ray detector for neurovascular interventions," *Conf. Proc. IEEE Eng. Med. Biol. Soc. 2011*, 7787–7790 (2011).
[90]L. Z. Leng, D. G. Rubin, A. Patsalides, and H. A. Riina, "Fusion of intraoperative three-dimensional rotational angiography and flat-panel detector computed tomography for cerebrovascular neuronavigation," World Neurosurg. (to be published).
[91]G. C. Kagadis *et al.*, "Computational representation and hemodynamic characterization of in vivo acquired severe stenotic renal artery geometries using turbulence modeling," Med. Eng. Phys. **30**, 647–660 (2008).
[92]B. J. Wood *et al.*, "Navigation systems for ablation," J. Vasc. Interv. Radiol. **21**, S257–263 (2010).
[93]J. Yoo, S. Schafer, A. Uneri, Y. Otake, A. J. Khanna, and J. H. Siewerdsen, "An electromagnetic "Tracker-in-Table" configuration for X-ray fluoroscopy and cone-beam CT-guided surgery," Int. J. Comput. Assist. Radiol. Surg. (to be published).
[94]Z. Yaniv, E. Wilson, D. Lindisch, and K. Cleary, "Electromagnetic tracking in the clinical environment," Med. Phys. **36**, 876–892 (2009).
[95]J. Borgert *et al.*, "Respiratory motion compensation with tracked internal and external sensors during CT-guided procedures," Comput. Aided Surg. **11**, 119–125 (2006).
[96]J. Krucker *et al.*, "Clinical utility of real-time fusion guidance for biopsy and ablation," J. Vasc. Interv. Radiol. **22**, 515–524 (2011).
[97]E. B. Levy, J. Tang, D. Lindisch, N. Glossop, F. Banovac, and K. Cleary, "Implementation of an electromagnetic tracking system for accurate intrahepatic puncture needle guidance: Accuracy results in an in vitro model," Acad. Radiol. **14**, 344–354 (2007).
[98]S. C. Gebhart, E. D. Jansen, and R. L. Galloway, "Dynamic, three-dimensional optical tracking of an ablative laser beam," Med. Phys. **32**, 209–220 (2005).
[99]T. He *et al.*, "A minimally invasive multimodality image-guided (MIMIG) system for peripheral lung cancer intervention and diagnosis," Comput. Med. Imaging Graph. **36**, 345–355 (2012).
[100]J. B. Stiehl and D. A. Heck, "Computer-assisted surgery: Basic concepts," Instr. Course Lect. **57**, 689–697 (2008).
[101]Y. Haga, T. Mineta, K. Totsu, W. Makishi, and M. Esashi, "Development of active catheter, active guide wire and micro sensor systems," Interv. Neuroradiol. **7**, 125–130 (2001).
[102]V. Kallem and N. J. Cowan, "Image guidance of flexible tip-steerable needles," IEEE Trans. Robot. **25**, 191–196 (2009).
[103]M. Brunelli *et al.*, "Influence of the anatomic characteristics of the pulmonary vein ostium, the learning curve, and the use of a steerable sheath on success of pulmonary vein isolation with a novel multielectrode ablation catheter," Europace **14**, 331–340 (2012).
[104]P. Kanagaratnam, M. Koa-Wing, D. T. Wallace, A. S. Goldenberg, N. S. Peters, and D. W. Davies, "Experience of robotic catheter ablation in humans using a novel remotely steerable catheter sheath," J. Interv. Card. Electrophysiol. **21**, 19–26 (2008).
[105]M. Mahvash and M. Zenati, "Toward a hybrid snake robot for single-port surgery," *Conf. Proc. IEEE Eng. Med. Biol. Soc. 2011*, 5372–5375 (2011).
[106]E. Florin, H. S. Rangwala, and S. Rudin, "Method to rotate an endovascular device around the axis of a vessel using an external magnetic field," Med. Phys. **34**, 328–333 (2007).
[107]C. V. Riga, C. D. Bicknell, D. Wallace, M. Hamady, and N. Cheshire, "Robot-assisted antegrade in-situ fenestrated stent grafting," Cardiovasc. Intervent Radiol. **32**, 522–524 (2009).
[108]H. Tillander, "Selective angiography of the abdominal aorta with a guided catheter," Acta Radiol. **45**, 21–26 (1956).
[109]S. Ramcharitar, M. S. Patterson, R. J. van Geuns, C. van Meighem, and P. W. Serruys, "Technology insight: Magnetic navigation in coronary interventions," Nat. Clin. Pract. Cardiovasc. Med. **5**, 148–156 (2008).
[110]J. K. Chun *et al.*, "Remote-controlled catheter ablation of accessory pathways: results from the magnetic laboratory," Eur. Heart J. **28**, 190–195 (2007).

[111] S. Ernst *et al.*, "Initial experience with remote catheter ablation using a novel magnetic navigation system: Magnetic remote catheter ablation," Circulation **109**, 1472–1475 (2004).
[112] B. L. Nguyen, J. L. Merino, and E. S. Gang, "Remote navigation for ablation procedures – A new step forward in the treatment of cardiac arrthymias," Eur. J. Cardiol. **6**, 50–56 (2010).
[113] M. S. Grady *et al.*, "Experimental study of the magnetic stereotaxis system for catheter manipulation within the brain," J. Neurosurg. **93**, 282–288 (2000).
[114] M. S. Grady *et al.*, "Magnetic stereotaxis: A technique to deliver stereotactic hyperthermia," Neurosurgery **27**, 1010–1015 (1990).
[115] M. S. Grady, M. A. Howard III, J. A. Molloy, R. C. Ritter, E. G. Quate, and G. T. Gillies, "Nonlinear magnetic stereotaxis: Three-dimensional, in vivo remote magnetic manipulation of a small object in canine brain," Med. Phys. **17**, 405–415 (1990).
[116] M. Schiemann, R. Killmann, M. Kleen, N. Abolmaali, J. Finney, and T. J. Vogl, "Vascular guide wire navigation with a magnetic guidance system: Experimental results in a phantom," Radiology **232**, 475–481 (2004).
[117] B. J. Wood *et al.*, "Navigation with electromagnetic tracking for interventional radiology procedures: A feasibility study," J. Vasc. Interv. Radiol. **16**, 493–505 (2005).
[118] K. Tsuchida *et al.*, "Guidewire navigation in coronary artery stenoses using a novel magnetic navigation system: First clinical experience," Catheter Cardiovasc. Interv. **67**, 356–363 (2006).
[119] K. Tsuchida *et al.*, "Feasibility and safety of guidewire navigation using a magnetic navigation system in coronary artery stenoses," EuroIntervention **1**, 329–335 (2005).
[120] F. Kiemeneij, M. S. Patterson, G. Amoroso, G. Laarman, and T. Slagboom, "Use of the Stereotaxis Niobe magnetic navigation system for percutaneous coronary intervention: Results from 350 consecutive patients," Catheter Cardiovasc. Interv. **71**, 510–516 (2008).
[121] G. Strassmann *et al.*, "Advantage of robotic needle placement on a prostate model in HDR brachytherapy," Strahlenther. Onkol. **187**, 367–372 (2011).
[122] S. Tovar-Arriaga, R. Tita, J. C. Pedraza-Ortega, E. Gorrostieta, and W. A. Kalender, "Development of a robotic FD-CT-guided navigation system for needle placement-preliminary accuracy tests," Int. J. Med. Robot. **7**, 225–236 (2011).
[123] K. Cleary, A. Melzer, V. Watson, G. Kronreif, and D. Stoianovici, "Interventional robotic systems: Applications and technology state-of-the-art," Minimally Invasive Ther. Allied Technol. **15**, 101–113 (2006).
[124] G. Fichtinger, P. Kazanzides, A. M. Okamura, G. D. Hager, L. L. Whitcomb, and R. H. Taylor, "Surgical and Interventional Robotics: Part II: Surgical CAD-CAM Systems," IEEE Rob. Autom. Mag. **15**, 94–102 (2008).
[125] P. Kazanzides, G. Fichtinger, G. D. Hager, A. M. Okamura, L. L. Whitcomb, and R. H. Taylor, "Surgical and interventional robotics: Core concepts, technology, and design," IEEE Rob. Autom. Mag. **15**, 122–130 (2008).
[126] J. Yanof *et al.*, "CT-integrated robot for interventional procedures: Preliminary experiment and computer-human interfaces," Comput. Aided Surg. **6**, 352–359 (2001).
[127] N. Hungr, C. Fouard, A. Robert, I. Bricault, and P. Cinquin, "Interventional radiology robot for CT and MRI guided percutaneous interventions," Med. Image Comput. Comput. Assist. Interv. **14**, 137–144 (2011).
[128] T. Penzkofer *et al.*, "Robot arm based flat panel CT-guided electromagnetic tracked spine interventions: Phantom and animal model experiments," Eur. Radiol. **20**, 2656–2662 (2010).
[129] C. V. Riga, C. D. Bicknell, M. S. Hamady, and N. J. Cheshire, "Evaluation of robotic endovascular catheters for arch vessel cannulation," J. Vasc. Surg. **54**, 799–809 (2011).
[130] C. V. Riga, N. J. Cheshire, M. S. Hamady, and C. D. Bicknell, "The role of robotic endovascular catheters in fenestrated stent grafting," J. Vasc. Surg. **51**, 810–819 (2010).
[131] G. A. Antoniou, C. V. Riga, E. K. Mayer, N. J. Cheshire, and C. D. Bicknell, "Clinical applications of robotic technology in vascular and endovascular surgery," J. Vasc. Surg. **53**, 493–499 (2011).
[132] C. Riga, C. Bicknell, M. S. Hamady, and N. J. Cheshire, "Robotically-steerable catheters and their role in the visceral aortic segment," J. Cardiovasc. Surg. **52**, 353–362 (2011).
[133] C. Riga, C. Bicknell, N. Cheshire, and M. Hamady, "Initial clinical application of a robotically steerable catheter system in endovascular aneurysm repair," J. Endovasc. Ther. **16**, 149–153 (2009).
[134] J. Tong, J. Zhou, L. Liu, Z. Pan, and H. Yan, "Scanning 3D full human bodies using kinects," IEEE Trans. Vis. Comput. Graph. **18**, 643–650 (2012).

Erratum: "Emerging technologies for image guidance and device navigation in interventional radiology" [Med. Phys. 39(9), 5768–5781 (2012)]

George C. Kagadis[a)]
Department of Medical Physics, School of Medicine, University of Patras, Rion, GR 265 04, Greece

Konstantinos Katsanos
Department of Interventional Radiology, Guy's and St.Thomas' Hospitals, NHS Foundation Trust, King's Health Partners, London SE1 7EH, United Kingdom

Dimitris Karnabatidis
Department of Radiology, School of Medicine, University of Patras, Rion, GR 265 04, Greece

George Loudos
Department of Medical Instruments Technology, Technological Educational institute of Athens, Ag. Spyridonos Street, Egaleo GR 122 10, Athens, Greece

George Nikiforidis
Department of Medical Physics, School of Medicine, University of Patras, Rion, GR 265 04, Greece

William R. Hendee
Department of Radiology, Mayo Clinic, Rochester, Minnesota 55905

(Received 16 November 2012; accepted for publication 16 November 2012; published 4 January 2013)

[http://dx.doi.org10.1118/1.4769414]

The authors would like to report a typographical error in Acknowledgment section.[1] The acknowledgment states: "This research has been co-financed by the European Union (European Social Fund—ESF) and Greek national funds through the Joint Research and Technology Program between Greece and France (2009–2011)". The correct Acknowledgement is: "This research has been co-financed by the European Union (European Regional Development Fund—ERDF) and Greek national funds through the Joint Research and Technology Program between Greece and France (2009–2011)."

[a)]Author to whom correspondence should be addressed. Electronic addresses: gkagad@gmail.com and George.Kagadis@med.upatras.gr; Telephone: +30 2610 969146; Fax: +30 2610 969166.

[1]G. C. Kagadis, K. Katsanos, K. Karnabatidis, G. Loudos, G. C. Nikiforidis, and W. R. Hendee, "Emerging technologies for image guidance and device navigation in interventional radiology," Med. Phys. **39**(9), 5768–5781 (2012).

